International J. Soc. Sci. & Education
2015 Vol.5 Issue 2, ISSN: 2223-4934 E and 2227-393X Print

Designing a biosensor for determination of H_2O_2 by using silver electrode modified with CuO nano particles and catalase

By

[1]Sahar seyed hossein, [2]Laleh Hafizi and [3]Nahid ghaed amini
[1]Department of biology, Payam Noor University, Tehran, Iran
[2]Department of biology, Payam Noor University, Esfahan, Iran
[3]Department of biology payam noor university, Esfahan,Iran

Abstract

In this study, we introduced a new biosensor for measurement of hydrogen peroxide (H2O2) by using of Catalase enzyme, Copper oxide nanoparticles and silver electrode. Copper oxide nanoparticles catalyze the redox protein Catalase enzyme and therefore facilitate the electron transfer between the silver electrode surface and the redox protein. Copper oxide nanoparticles have been synthesized in the laboratory, were studied by using a variety of chemical spectrum UV – Vis, XRD, SEM and TEM. XRD confirmed that using our synthesis are of copper oxide nanoparticles. Nanoparticles showed Absorption spectrophotometry at 265 nm and thus nanoparticles showed the quantum properties. SEM and TEM showed that nanoparticles were to form spherical and have size 35 - 45 nm. Direct electrochemistries of Catalase enzyme with the use of these nanoparticles were easily. And a pair of semi-reversible redox peaks shown of Fe(II) and Fe(III) with the formal potential (E °) -0/1995*V electrode against a silver /silver chloride (Ag / Ag cl) at pH = 7 and 0.1M phosphate baffer . Designed sensor has high sensitivity and short response time (<7sec), and in linear range of 25μM to 800 μM can be used to determine hydrogen peroxide. This biosensor also has very good stability.*

Keywords: *Biosensor, Hydrogen peroxide, Catalase enzyme ,Copper oxide nanoparticles, silver electrode electrode*.

1. Introduction

Nanotechnology is a relatively new and vast field. The increased presence of nanomaterials in commercial products such as cosmetics and sunscreens, dental fillings, photovoltaic cells, and water filtration and catalytic systems has resulted in a growing public debate on the oxicological and environmental effects of direct and indirect exposure to these materials[1-2]. At present, these effects are not completely elucidated. Nanotechnology involves the ailoring of materials at atomic level to attain unique properties, which can be suitably manipulated for the desired applications [3-5]. Most of the natural processes also take place in the nanometer scale regime. Therefore, a confluence of nanotechnology and biology can address several biomedical problems, and can revolutionize the field of health and medicine [6]. Nanotechnology is currently employed as a tool to explore the darkest avenues of medical sciences in several ways like imaging [7], sensing [8], targeted drug delivery [9] and gene delivery systems [10] and artificial implants [11]. Sensors are the devices, which are composed of an active sensing material with asignal transducer[12-14].

The role of these two important components in sensors is to transmit the signal without any amplification from a selective compound or from a change in a reaction. These devices produce any one of the signals as electrical, thermal or optical output signals that could be converted in to digital signals for further processing[15]. One of the ways of classifying sensors is done based on these output signals. Among these, electrochemical sensors have more advantage over the others because; in these, the electrodes can sense the materials, which are present within the host without doing any damage to the host system. On the other hand,sensors can be broadly classified in to two categories as chemical sensors and iosensors. The biosensors can be defined in terms of sensing aspects, where these sensors can sense biochemical compounds such as biological proteins, nucleotides and even tissues [16-19]. The history of biosensors

started in 1962 with the development of enzyme electrodes by scientist Leland C. Clark[20]. Since then, research communities from various fields such as very large scale integration (VLSI), physics, chemistry, and material science have come together to develop more sophisticated, reliable, and mature biosensing devices[21].

Applications for these devices are in the fields of medicine, agriculture, biotechnology as well as the military and bioterrorism detection and prevention. Cadmium oxide is attracting tremendous attention due to its interesting properties like direct band gap of 2.3 eV. It is widely used in the applications like the preparation of cadmium-coated baths and anufacture of paint pigments. Cadmium sulphide is one of the most studied materials with a band gap of 2.43eV. It is primarily used in solar cell and a variety of electronic devices[22].

The photoconductive and electroluminescent properties of cadmium sulphide have been applied in manufacturing a variety of consumer goods. In the present paper, synthesis and characterization of cadmium oxide and cadmium sulphide nanoparticles has been studied that used as facile electron transfer[23].

Enzymes are biological catalysts in the form of proteins that catalyze chemical reactions in the cells of living organisms. As such, they have evolved – along with cells – under the conditions found on planet Earth to satisfy the metabolic requirements of an extensive range of cell types[24]. Catalases are some of the most efficient enzymes found in cells. Each catalase molecule can decompose millions of hydrogen peroxide molecules every second. The cow catalase shown here (PDB entry 8 cat) and our own catalases use an iron ion to assist in this speedy reaction[25-27].

The enzyme is composed of four identical subunits, each with its own active site buried deep inside. The iron ion, shown in green, is gripped at the center of a diskshaped heme group[28]. Catalases, since they must fight against reactive molecules, are also unusually stable enzymes. Notice how the four chains interweave, locking the entire complex into the proper shape. Catalase is an important enzyme of oxidoreductase family, which has been widely employed in biosensors for sensitive and selective H2O2 determination [29].

However, the selection of suitable electrode material and novel immobilization matrices with good electronic properties is essential to enhance the direct electron transfer between Catalase and the electrode surfaces.

Previous studies emphasis the key roles played by the anomaterials in promoting the direct electrochemistry of Catalase [30-32]. In this paper, we investigated electrochemical behavior of catalase enzyme by use of silver electrode and, Copper oxide The reduction reactions of mentioned electrochemical behavior used as hydrogen peroxide (H_2O_2) biosensor.

2. Materials and Methods

Catalase from bovine liver (40-45 units/ mg) was purchased from Sigma. The phosphate buffer solution (PBS) consisted of a potassium phosphate solution (KH2PO4 and K2HPO4 from Merck; 0.1 M total phosphate) at pH 7.0.

All other chemicals were of analytical grade and were used without further purification. All solutions were made up with doubly distilled water.

Apparatus

Cyclic voltammetric experiments were performed with a model EA-201 Electro Analyzer (chemilink systems),equipped with a personal computer was used for electrochemical measurement and treating of data.

A conventional three electrode cell was employed throughout the experiments, with bare or Copper oxide nanoparticles modified silver paste electrode (5.0 mm diameter) as working electrode, a saturated calomel electrode (SCE) as a reference electrode and a platinum electrode as a counter electrode. The phase characterization was performed by means of Xray diffraction (XRD) using a D/Max-RA diffractometer with CuK radiation. Samples were measured and recorded using a TU-1901 double-beam UV–visible spectrophotometer were dispersed in toluene solution.

Preparation methods

Cu=O nanostructures with different sizes and shapes morphology were obtained by sonochemical method using copper(II) acetate as precursors, urea and sodium hydroxide as reducing agent and polyvinylpyrrolidone (PVP) as stabilizing polymer, followed by irradiation using high-intensityultrasound [33]. Monoclinic phase CuO-NPs were obtained with quasi-spherical microarchitectures and long-straw like structures when using urea and sodium hydroxide, respectively.

Experimental section

All of the reagents used in the experiment were of analytic purity. Figure 1 shows the preparation process. The synthesis process is based on the following chemical reactions in solution:

Cu2 NaOH Cu OH Na
2 2 2 + + = ( ) + + (1)
Cu(OH)2 □ CuO + H2O (2)

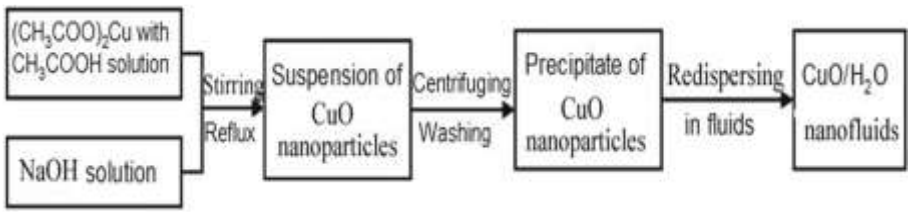

Figure 1 Preparation process of CuO aqueous nanofluids.

In a typical procedure, 600 ml 0.2 M copper acetate(Cu(CH3COO)2·H2O) solution and 2 ml glacial aceticacid H3COOH) were added into a round-bottomed flask and heated to boiling under magnetic stirring.

Then, 30 ml 8 M sodium hydroxide (NaOH) solutionwas poured into the flask. The color of the solution turned from blue to black immediately, and a black suspensionformed simultaneously.

The reaction was carried out under stirring and boiling for 2 h. The mixture was cooled to room temperature and centrifuged.

Then,a wet CuO precipitate was obtained. The wet precipitate was washed twice with distilled water to remove theimpurity ions.

CuO nanofluids of different volume fractions were obtained by re-dispersing the wet recipitate into different amounts of distilled water under ultrasonic vibration (120 W, 40 Hz).
To study the influences of synthesis parameters on the final products, the kinds and amounts of copper salts,reaction time were changed while keeping all other experimental parameters same as in the typical run.

The XRD pattern of the powder (obtained by drying the washed wet precipitate) was recorded on a Rigaku D/Max r-A diffractometer. TEM images were captured on a JEM-2000EX instrument. The nanofluids were diluted with distilled water and dispersed by ultrasonic.Then, one drop was placed on a carbon-coated copper grid and left to dry at room temperature. Particle size distributions of the nanoparticles in nanofluids were measured with a Zetasizer 3000HS (Malvern) particle size analyzer.

The samples were also prepared by diluting the nanofluids with distilled water and dispersed by ultrasonic. Thermal conductivity was measured using a KD2 Pro Thermal Property Analyzer (Decagon Inc.,Pullman, WA, USA) based on the transient hot wire method.

The nanofluids were sonicated for about 30 min before measurements so that the samples would have the same dispersity.

Characterization of typical sample

Figure 2a is the XRD pattern of the typical sample. All the peaks on the XRD pattern can be indexed to that of monoclinic CuO according to the literature (JCPDS, FileNo 80-1916). The average crystal size is 36 nm alculated using Debye-Scherrer formula. Figure 2d shows a TEM image of the typical sample. The size of primary particles is about 36 nm, which is in good agreement with the result of XRD.

The primary particles aggregate to chain-like clusters with width of 36 nm and length of 50-150 nm (5-15 primary particles). Figure 2c is the size distribution of the typical sample.

The particle size is about 20-80 nm, and the size distribution is narrow.The larger particle size is due to the short clusters shown in the TEM image. The obtained CuO nanofluids could remain stable for 5 months with no visible precipitation at the bottom.

Influences of copper salts

By replacing Cu(CH3COO)2·H2O with CuCl2·2H2O and Cu(NO3)3·3H2O, respectively, different CuO nanofluids were prepared with all other experimental parameters unchanged. Figure 3 is the TEM images of above two nanofluids. When using CuCl2·2H2O as copper source (Figure 3a), the obtained particles in nanofluids are flake-like particles with width of 34-45 nm and length of 100-300 nm. When using Cu(NO3)2·3H2O (Figure 3b),the particles are aggregations of thin sticks and particles of about 15-50 nm. It has been approved by some researchers that the anions could affect the growth orientation and process of nanoparticles by adsorption or coordination interaction of anions with special crystal face of particles [34]. Therefore, by changing copper source, we could obtain particles with different morpholog .

Influences of copper acetate concentration

Figure 4a,b are the TEM images of CuO nanofluids prepared with copper acetate concentration of 0.1 and 0.4 mol·l-1, respectively. Compared with typical nanofluids (obtained with concentration of 0.2 mol·l-1), it is clear that the size of primary nanoparticles remain almost the same (about 36 nm), but the morphology and size of nanoparticles cluster change with copper acetate concentration. When the concentration is 0.1 mol·l-1, the clusters are also chain-like structures with lengths in the range of 100-200 nm. It is longer than the clusters in typical samples. When the concentration is 0.4 mol·l-1, the primary nanoparticles aggregate and form irregular clusters consisted of 2-30 primary nanoparticles. The formation of chain-like cluster may be due to the orientation adhesion mechanism [35].

When the concentration of copper acetate is low, the collision probability of primary CuO nanoparticles is low; thus, the orientation adhesion is preponderant in the reaction process. Therefore, by changing the concentration of copper acetate, the size and structure of cluster could be adjusted.

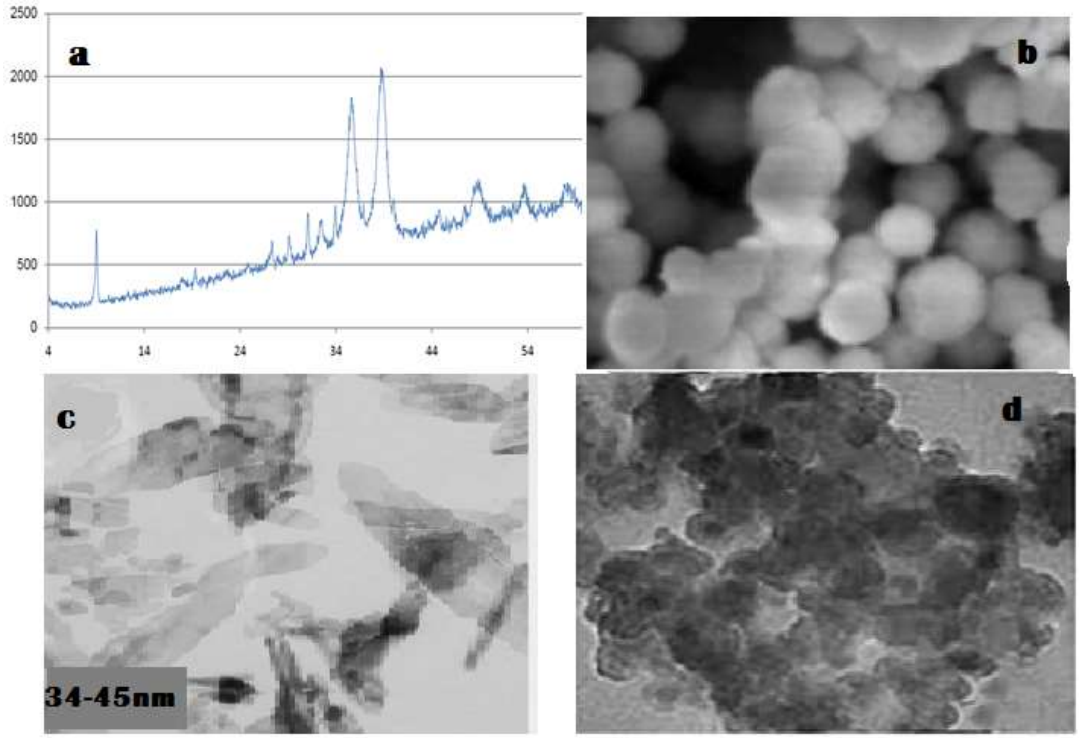

Figure 2 Characterization of the typical sample. (a) XRD pattern; (b)SEM image; (c) size distribution; (d)TEM image.

Influence of reaction time

Figure 5 is the TEM images of CuO nanofluids obtained with different reaction times. When the reaction time is 12 h (Figure 5a), average size of CuO primary nanoparticles is about 36 nm. CuO nanoparticles form flexural chains consisting of 30-50 primary particles. It is longer than the chain in typical sample (Figure 2b).

When the reaction time was increased to 25 h (Figure 5b), the size of the primary particles is also about 36 nm, but the chain-like clusters do not exist any more. Instead, there are small aggregates composed of several primary particles. As mentioned above, the formation mechanism of chain-like cluster is orientation adhesion. With the increase of reaction time, the orientation adhesion degree increases; and thus, the length of the cluster increases. \

Why do the chain-like clusters destroy when the reaction time is 25 h(Figure 5c), It needs more detailed research in future studies. The above results show that different microstructures could be obtained through changing the reaction time.

Thermal conductivity of CuO nanofluids

Figure 6 shows the thermal conductivity ratio of the typical sample, defined as k/k0, where k and k0 are the thermal conductivities of the nanofluids and the base media (H2O) respectively, as a function of the particle volume fraction at 25°C.

The thermal conductivity of the base fluid (H2O) was measured, and it had an average value of 0.580 W·m-1·K-1. It can be seen that the thermal conductivity ratio increases as the particle volume fraction increases.

This is in good agreement with some research, in which the thermal conductivity of nanofluids also increase linearly with the particle loading [36,37]. On comparing with some reported experimental results of CuO nanofluids, the current data are found to be close to Lee et al.'s data, Das et al.'s data, and Liu et al.'s data [38-40], suggesting the potential application as heat transfer fluids.

Figure 3 TEM images of CuO nanofluids prepared with different copper salts. (a) CuCl2·2H2O; (b) Cu(NO3)2·3H2O.

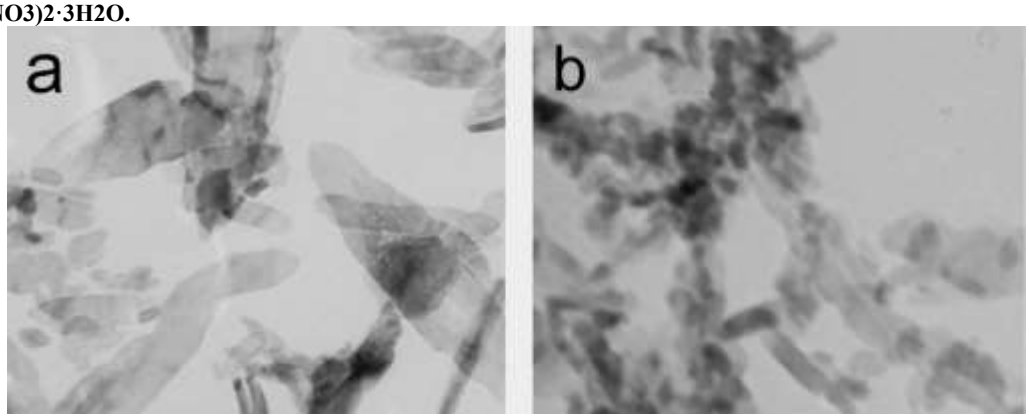

Figure 4 TEM images of CuO nanofluids prepared with different concentrations of (CH3COO)2Cu·H2O solution. (a) 0.1 mol·l-1;(b) 0.4 mol·l

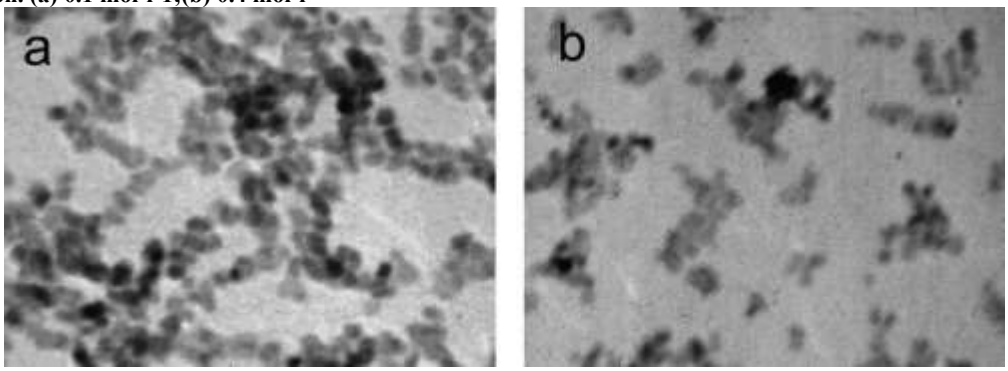

Figure 5 TEM images of CuO nanofluids synthesized under different reaction times. (a) 12 h; (b) 25 h.

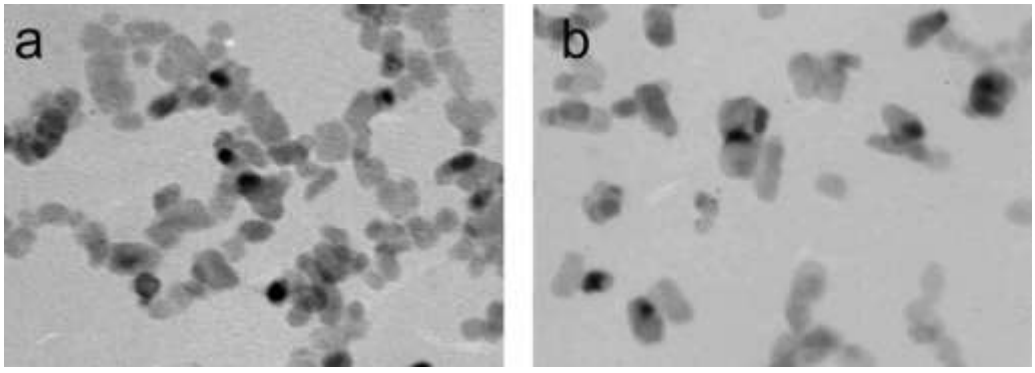

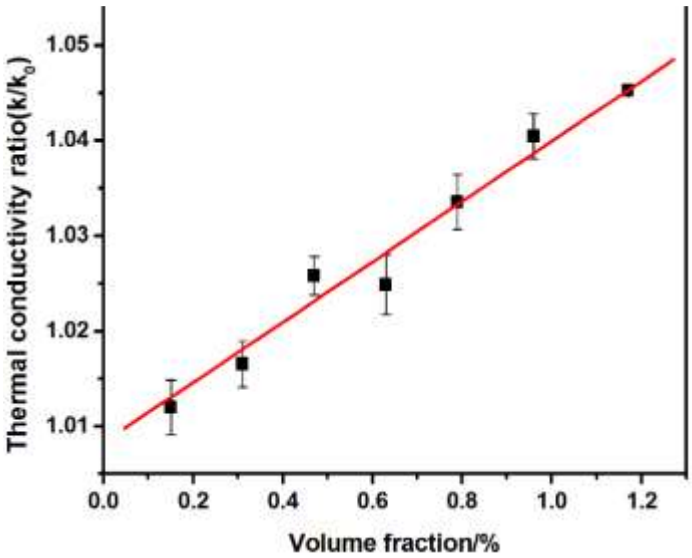

Figure 6 Thermal conductivity ratio as a function of CuO volume fraction at 25°C.

A wet chemical method to synthesize stable CuO nanofluids in a large-scale was developed successfully. The influences of synthesis parameters on nanofluids microstructures were investigated. Different copper salts resulted in different particle morphologies. The concentration of copper acetate and reaction time affected the size and shape of clusters of primary nanoparticles.

Nanofluids with different microstructures could be obtained through changing the synthesis parameters. The thermal conductivity of CuO nanofluids increased with the increase of particle loading. It is expected that this method can be extended to synthesize other nanofluids.

UV–visible absorption spectra for CuO nanoparticles

The UV–visible absorption spectra of CuO nanoparticles was shown in Fig.7; although the wavelength of our spectrometer is limited by the light source, the absorption band of the CuO nanoparticles have been shows a blue shift due to the quantum confinement in sample compare with bulk CuO particles. This optical phenomenon indicates that these nanoparticles show quantum size (265nm)effect.

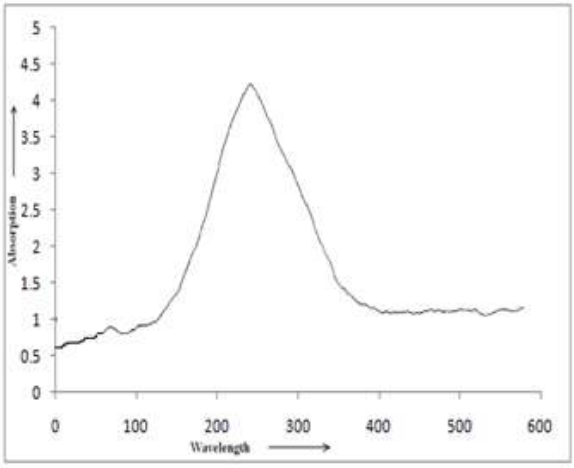

Figure 7. UV-Absorption spectra for CuO nanoparticles

Direct voltammetric behavior of the CAT/CUo/ silver paste electrode

The integrity of the immobilized catalase construction and its ability to exchange electrons with the nanometerscale Cuo particles surfaces were assessed by voltammetry.

A macroscopic electrode was required to attain a large enough catalase sample to yield detectable direct oxidation and reduction currents. The comparative CVs for the Cuo/ NPs and CAT / Cuo NPs/ silver electrodes in 0.1 M PBS (pH 7.0) were obtained. These voltammograms are demonstrated in Fig. 8 (a,b).

From this Figure, it was noticed that there were no ltammetric response on Cuo NPs/silver paste electrode (Fig. 8a), which, Fig. 8(b) depicts a well-defined pair of oxidation–reduction (redox) peaks, observed on the CAT / Cuo NPs silver paste electrode at 100 mv/s scan rate value.

The CAT / Cuo NPs/ silver paste electrode presented the reductive peak potential at -221 V and the corresponding oxidative peak potential at -178 V (at 100 mV s-1), illustrating the adsorbed catalase on the nanometer-scale copper oxide particle surfaces.

The difference of anodic and cathodic peak potential values was DE = -43 V. These redox peaks were attributed to the redox reaction of the catalase electroactive center. The formal potential (E0) for the catalase redox reaction on the CAT / Cuo NPs/ silver paste electrode was- 0/1995 V with respect to the reference electrode.

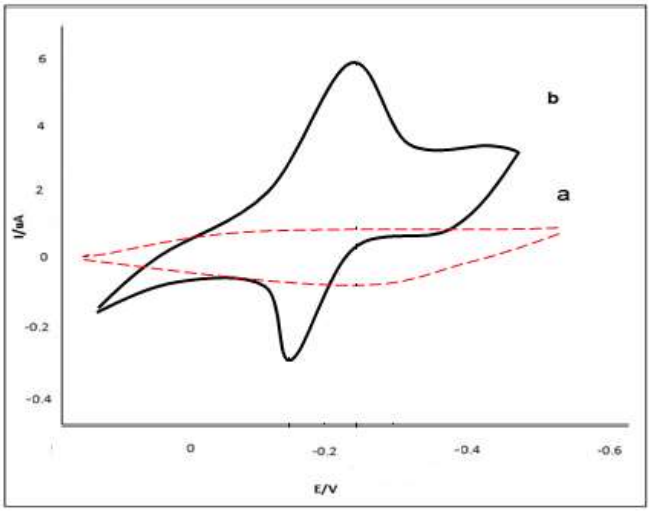

Figure8.Cyclic voltammograms, using (a) the CAT/silver electrode in 0.1 M phosphate buffer and (b CAT / CuONPs/ silver electrode in 0.1 M phosphate buffer (scan rate: 100 V/s).

The collected voltammograms in Fig. 8 (a), substantiated this statement that the nanometer-scale cadmium oxide particles could play a key role in the observation of the catalase CV response. On the grounds that the surface-to volume ratio increases with the size decrease and because of the fact that the enzyme size is comparable with the nanometer-scale building blocks, these nanoparticles displayed a great effect on the electron exchange assistance between catalase and silver paste electrode. To further investigate the catalase characteristics at the CAT/CuO NPs/ silver electrode, the effect of scan rates on the catalase voltammetric behavior was studied in detail.

The baseline subtraction procedure for the cyclic voltammograms was obtained in accordance with the method reported by Bard and Faulkner [41].

The scan rate (ν) and the square root scan rate (ν1/2) dependence of the heights and potentials of the peaks are plotted in Fig. 8(b) and Fig. 8 (c) respectively. It can be seen that the redox peak currents increased linearly with the scan rate, the correlation coefficient was 0.9973 (ipc = 0.992ν) and 0.9999 (ipa = 0.997 ν), respectively. This phenomenon suggested that the redox process was an adsorption-controlled and the immobilized catalase was stable. In Fig. 8(c) It can be seen that the redox peak currents increased more linearly with the 0.2ν in comparison to that of ν0.7.

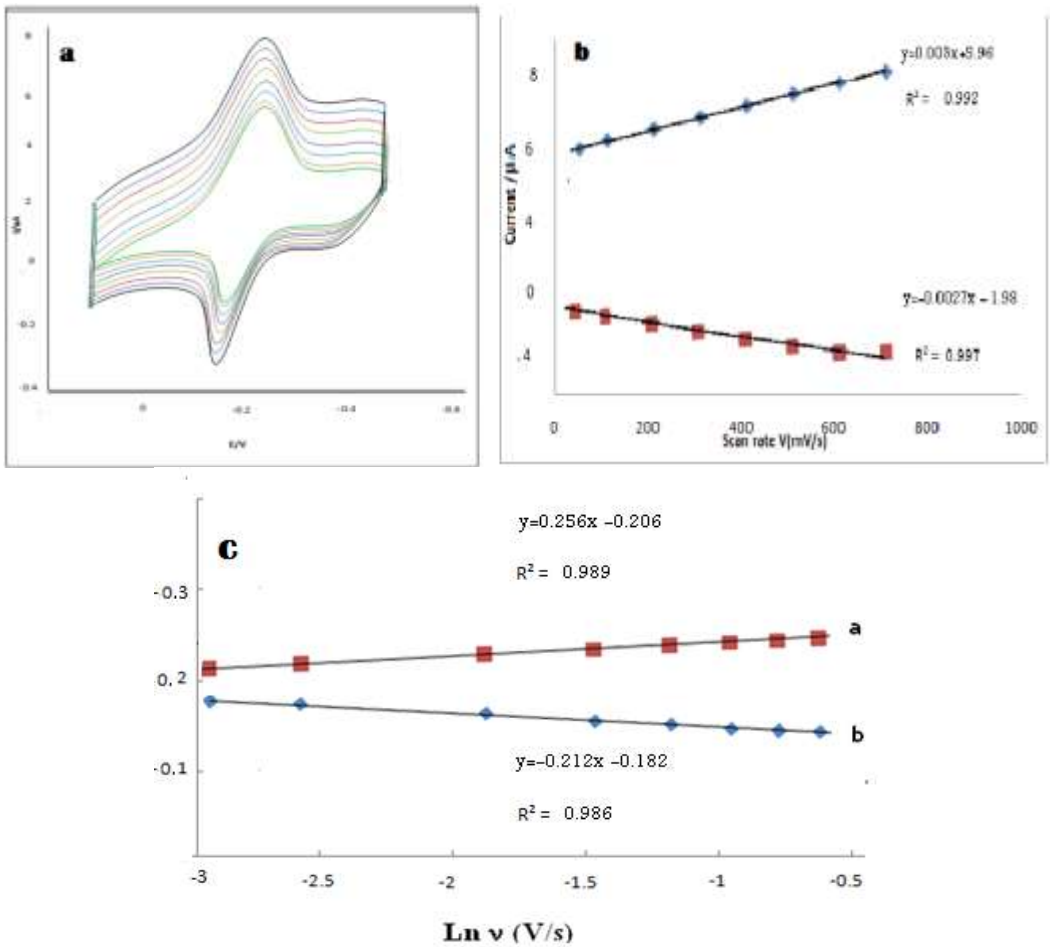

Figure.9. (a) CVs of CAT / CuO NPs/ silver electrode in PBS at various scan rates, from inner to outer; 100,200, 300,400,500,600and 700 mV s-1, the relationship between the peak

However, there is clearly a systematic deviation from linearity in this data, i.e. low scan rates are always on one side of the line and the high scan rate points are on the other.

The anodic and cathodic peak potentials are linearly dependent on the logarithm of the scan rates (ν) when ν > 0.2 V s-1, which was in agreement with the Laviron theory, with slopes of -2.3RT/anF and 2.3RT/ (1 -a) nF for the cathodic and the anodic peak, respectively [36]. So,the charge-transfer coefficient (a) was estimated as 0.49. Furthermore, the heterogeneous electron transfer rate constant (ks) was estimated according to the following equation [36,37]:

[log ks = a log(1-a) + (1-a) loga - log -] (1)

Here, n is the number of transferred electrons at the rate of determining reaction and R, T and F symbols having their conventional meanings. The average heterogeneous transfer rate constant (ks) value was calculated about, 1.937s-1.

Electrocatalytic reduction of H2O2 on the CAT/Cuo NPs/ silver retained electrode

Upon addition of H2O2 to 0.1M pH 7.0 PBS, the cyclic voltammogram of the CAT/Cuo NPs/ silver electrode for the direct electron transfer of catalase changed dramatically with an increase of reduction peak current and a decrease of oxidation peak current (Fig. 10a), while the change of cyclic voltammogram of bare or Cuo Nps/ silver was negligible (not shown), displaying an obvious electrocatalytic behavior of the catalase to the reduction of H2O2.

The decreases of the oxidative peak current together with the increases of the reductive CAT/Cuo NPs/silver.

The electro-catalytic process could be expressed as follows:

CAT-Fe (III) + e- + H+ ↔ CAT -Fe (II) H+ at the electrode surface (2)

H_2O_2 + CAT-Fe (II) H+ → CAT-Fe (III) + H+ + H_2O_2 in the solution (3)

Calibration curve (Figure 5b) shows the linear dependence of the cathodic peak current on the H_2O_2 concentration in the range of 25 to 800 μM. In Figure 5 b, at higher concentration of H_2O_2, the cathodic peak current decreased and remains constant. Upon addition of an aliquot of H_2O_2 to the buffer solution, the reduction current increased steeply to reach a stable value (Fig 10 b). This implies electro catalytic property of electrode. Thus, this experiment has introduced a new biosensor for the sensitive determination of H_2O_2 in solution.

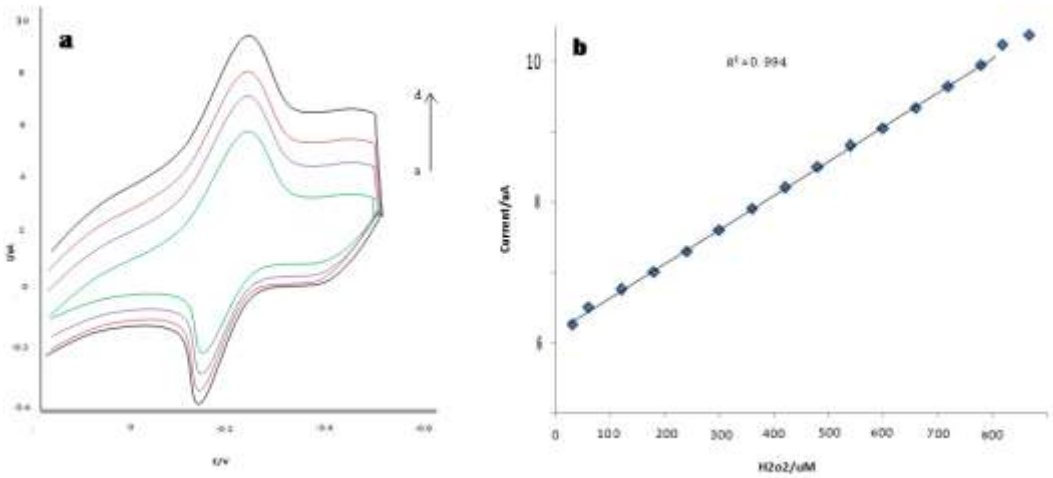

Figure .10. (a) Cyclic voltammograms obtained at an CAT / CuO NPs/ silver in 0.1M phosphate buffer solution (pH 7.0) for different concentrations of and (b) the relationship between cathodic peak current of CAT and different concentrations of H2O2 (scan rate: 100 mVs-1).

Effect of temperature on the H2O2 sensor

Temperature is an important parameter affecting the electrocatalytic activity of enzyme or protein. Fig. 11 shows the effect of temperature on sensor response. With an increasing temperature from 7 oC to 52 oC the response and the electrocatalytic activity of the immobilized catalase increased.The immobilized catalase had activity even at 52 oC.It was evident that the immobilized catalase had good thermal stability because of the unchanged ability of microenvironment and its native structure upon temperature change.

These results indicated that this sensor could handle in a wide range of temperature, but it has maximum of response only at 22-31oC.

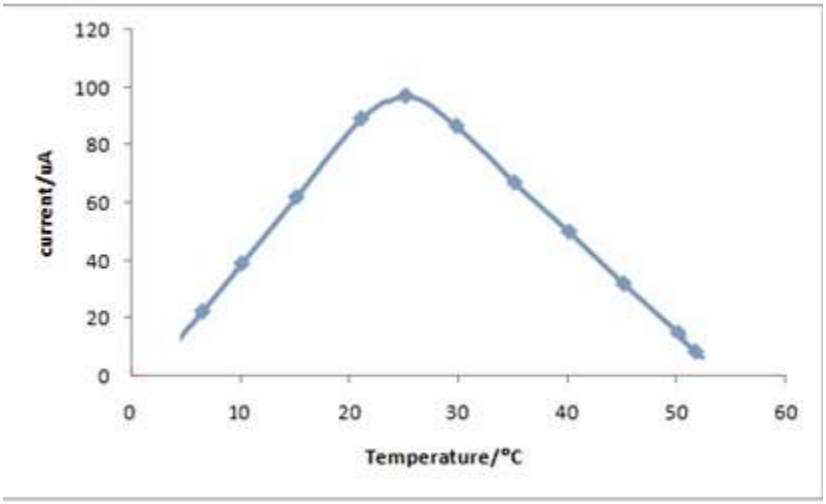

Figure11. Effect of temperature on biosensor at pH 7.0.

Stability of the H2O2 biosensor

The stability of CAT / CuO NPs/ silver electrode biosensor has been checked by carrying out experiments at the regular interval of a week and it has been found that CAT / CuO NPs/ silver electrode based electrochemical biosensor retains its 85% activity after 30 days. The loss in the activity of biosensor is not due to the denaturation of catalase but it is due to the poor adhesion of copper oxide Nanoparticles on the silver paste electrode.

For a result, interface materials have not high effect on operation of this biosensor. Undoubtedly, nanotechnology in combination with bioelectrochemistry can extremely influence the development rate of these scientific fields[10-12].

However, a number of challenges remain to be faced, which are related to the processing of the electrode modifications in a more controlled method. The charge transport mechanism in the nanostructured biointerfaces presents a great interest, requiring further investigation. Nevertheless, the recent advances have been important for the comprehension of the nanostructured biointerfaces. As a result, it will be possible to study the modern material sciences, including bioelectronics, biocatalysis and biosensing.

Conclusion

Silver paste electrodes modified with nanoparticles of copper oxide were employed for the electrocatalytic reduction and determination of hydrogen peroxide.

Catalase can be effectively immobilized on copper oxide nanoparticles modified silver paste electrode to produce a fast direct electron transfer. The immobilized catalase maintains its bioactivity and native structure. The combination of catalase enzyme and Cuo NPs in the biosensor would result in the improvement of analytical performance, characterized by broader linear range and lower detection limit for H2O2 determination. Moreover, the biosensor possesses good stability and reproducibility, and achieves 85% of the steady state.

References

[1] Benhar, I., Eshkenazi I., Neufeld, T., Opatowsky, J., Shaky, S., and Rishpon, J. Talanta, 2001, 55, 899–907.
[2] Bertozzi, C.R., and Kiessling, L.L, Chemical Glycobiology. Science, 2001, 291, 2357–2364.
[3] Brandt, O., and Hoheisel, J.DTrends Biotechnol, 2004, 22, 617–622.
[4] Cardullo, F., Diederich, F., Echegoyen, L., Habicher, T., Jayaraman, N., Leblanc, R.M., Stoddart, J.F., and Wang, S. Langmuir, 1998, 14, 1955–1959.
[5] Emanuel, P.A., Dang, J., Gebhardt, J.S., Aldrich, J., Garber, E.A.E., Kulaga, H., Stopa, P, Valdes, J.J., and Dion-Schultz, ABiosens. Bioelectron, 2000, 14, 751–759.
[6] J. B. Raoof, Ojani, and A. Kiani, J. Electroanal. Chem, 2001, 515, 45
[7] D. R. Shankaran, K. Limura, T. Kato, Sens, Actuators, B, Chem, 2003, 94 73.
[8] J. W Mo, B. Ogoreve. Anal Chem, 2001,73, 1196.
[9] R. Thanavelan, G. Manikandan, G. Ramalingam, V. Thanikachalam, Der Chemica Sinica, 2011, 2, 4, 90-98.
[10] H P Klug, L E Alexander, Wiley, New York, 1954.
[11] Haiming Fan, Lintao Yang, Nanotechnology, 2004, 15, 37
[12] X. R. Ye, C. Daraio, C. Wang, J. B. Talbot, Jin Journal of Nanoscience and Nanotechnology, 2006, 6 ,852.
[13] E.A. Meulenkamp, J. Phys. Chem, 1998, 102, 7764.
[14] Gemeiner, P., Docolomansky, P., Vikartovska, A., and Stefuca, V, Biotechnol. Appl. Biochem. 1998, 28, 155–161.
[15] Majumdar, A., and Thundat, T, Anal. Chem, 2001, 73, 1567–1571.
[16] D.Nagarjuna Reddy, K.Vasudeva Reddy, T. Sreenivasulu Reddy and K. Hussain Reddy, Der Chemica Sinica, 2011, 2 , 4, 123-132.
[17] Subrahmanyam, S., Piletsky, S.A., and Turner, A.P.F, Anal. Chem, 2002, 74, 3942–3952.
[18] Sachin. V. Bangale, S. M. Khetre and S. R. Bamane, Der Chemica Sinica, 2011, 2, 4, 303-311.
[19] Tien, H.T.; Wurster, S.H.; Ottova, A.L. Bioelectrochem Bioenerg, 1997, 42, 77–94.
[20] K.M. Abd El-Salaam, E.A. Hassan, Surf Technol, 1982, 16, 121.
[21] D.G. Shchukin, D.V. Sviridov, A.I. Kulak, Sens Actuators, 76 (2001) 556.
[22] A. Gulino, G. Compagnini, A.A. Scalisi, Chem Mater, 2003, 15, 3332.
[23] R.S. Mane, H.M. Pathan, C.D. Lokhande, Sol. Energy, 2006, 80, 185.
[24] Birendra Pratap Singh, Jai Prakash Singh, Shruti Shukla , Shanti Sharma, Der Chemica Sinica, 2012, 3, 2, 521- 526.
[25] Holum, J, Elements of General and Biological Chemistry, 2nd ed., Wiley, NY ,1968, pp 377.
[26] Martinek, R, Practical Clinical Enzymology, J. Am. Med. Tech., 1969, 31, 162.
[27] Harrow, B., and Mazur, A, Textbook of Biochemistry, 1958, 108,109.
[28] D. K. Sawant, D. S. Bhavsar, Der Chemica Sinica, 2011, 2 ,4, 211-218.
[29] B. Zhou, J. Wang, X.Gao, Y. Tian, Anal. Lett, 2008, 41, 1832.
[30] L. Shen, N. Hu, Biomacromolecules, 2005, 6, 1475.
[31] K.J. Huang, .D.J. Niu, X. Liu, Z.W. Wu, Y. Fan, Y.F. Chang, Y.Y. Wu, Electrochim. Acta, 2011,56 , 2947.
[32] L. Staudenmaier, Ber. Dtsch. Chem. Ges, 1898, 31, 1481.
[33] Haiming Fan, Lintao Yang, Nanotechnology, 2004, 15, 37.
[34] X. R. Ye, C. Daraio, C. Wang, J. B. Talbot, Jin Journal of Nanoscience and Nanotechnology, 2006, 6 , 852.
[35] A. J. Bard and L. R. Faulkner, John Wiley & Sons, New York, NY, USA, 2nd edition., 2001,241.
[36] E. Laviron Journal of Electroanalytical Chemistry., 1979, 101, 1, 19-28.
[37] E. Laviron Journal of Electroanalytical Chemistry., 1979, 100, 263-270.
[33] Choi SUS: Enhancing thermal conductivity of fluids with nanoparticles. In Developments and Applications of Non-Newtonian Flows. Edited by: Singer DA, Wang HP. New York: American Society of Mechanical Engineers; 1995:99-105.

[34] Zhong WZ, Hua SK: Anion coordination polyhedra and crystal morphology. Morphology of Crystal Growth Beijing: Science Publisher; 1999, 114-126.
[35] Teo JJ, Chang Y, Zeng HC: Fabrications of hollow nanocubes of Cu2O and Cu via reductive self-assembly of CuO nanocrystals. Langmuir 2006, 22:7369-7377.
[36] Shima PD, Philip J, Raj B: Influence of aggregation on thermal conductivity in stable and unstable nanofluids. Appl Phys Lett 2010, 97:1531131-1531133.
[37] Philip J, Shima PD, Raj B: Evidence for enhanced thermal conduction through percolating structures in nanofluids. Nanotechnology 2008, 19:3057061-3057067.
[38] Lee S, Choi SUS, Li S, Eastman JA: Measuring thermal conductivity of fluids containing oxide nanoparticles. J Heat Transfer 1999, 121:280-289.
[40] Liu MS, Lin MCC, Huang IT, Wang CC: Enhancement of thermal conductivity with CuO for nanofluids. Chem Eng Technol 2006, 29:72-77.